

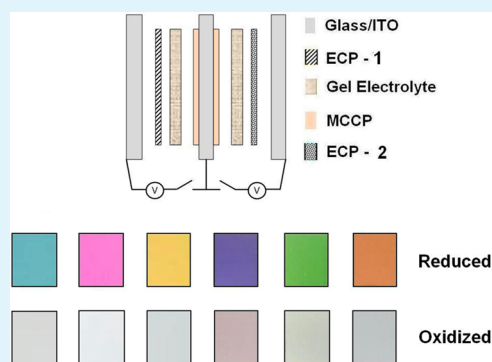
# Mapping the Broad CMY Subtractive Primary Color Gamut Using a Dual-Active Electrochromic Device

Rayford H. Bulloch, Justin A. Kerszulis, Aubrey L. Dyer, and John R. Reynolds\*

School of Chemistry and Biochemistry and School of Materials Science and Engineering, Center for Organic Photonics and Electronics, Georgia Institute of Technology, Atlanta, Georgia 30332, United States

## S Supporting Information

**ABSTRACT:** Although synthetic efforts have been fruitful in coarse color control, variations to an electrochromic polymer (ECP) backbone are less likely to allow for the fine control necessary to access the variations and shades of color needed in display applications. Through the use of thin films of cyan, magenta, and yellow ECPs, non-emissive subtractive color mixing allows the color of an electrochromic device (ECD) to be selected and tailored, increasing access to various subtle shades and allowing for a non-emissive display to exhibit a wide range of colors. Using a dual-active ECD, subtractive color mixing utilizing the cyan–magenta–yellow (CMY) primary system was examined. The bounds of the gamut, or the subset of accessible colors, using these three 3,4-propylenedioxythiophene (PProDOT)-derived materials in combination with the recently recognized 3,4-propylenedioxy pyrrole-based minimally color changing polymer (MCCP) were mapped, highlighting the benefit of applying subtractive color mixing toward the development of full-color non-emissive displays. Here, we demonstrate that ECPs are suitable for the generation of a wide gamut of colors through secondary mixing when layered as two distinct films, exhibiting both vibrantly colored and highly transmissive states.



**KEYWORDS:** electrochromism, electrochromic devices, color mixing, organic electronics, colorimetry, conjugated electroactive polymers

## INTRODUCTION

Through variations on a poly(3,4-propylenedioxy-thiophene) (PProDOT) polymer backbone, a family of electrochromic polymers (ECPs) spanning the breadth of the color palette have become available for study.<sup>1</sup> While maintaining the solubility of these materials that makes them amenable to processing techniques such as airbrush and ultrasonic spraying, slot-die coating, and spin casting, color has been varied through incorporation of moieties such as electron-rich groups, donor–acceptor monomer units, and modification of steric effects.<sup>2–6</sup> Among this family of ECPs are three polymers of particular note, namely, the ECPs that exhibit a magenta-, cyan-, or yellow-to-transmissive transition, referred to as ECP-M, ECP-C, and ECP-Y throughout this work, the structures of which are shown in Figure 1a. Each of these materials possesses the low oxidation potential characteristic of ProDOT-based polymers while maintaining the solution processability imparted through functionalization of the propylene bridge with 2-ethylhexyloxy chains. Considerable synthetic efforts have gone into developing ECPs representing each primary color.<sup>7</sup> Although these synthetic efforts have been fruitful in coarse color control, variations to a polymer backbone are less likely to allow for the fine control necessary to access the variations and shades of color needed in display-type applications. Through the use of thin films of cyan, magenta, and yellow ECPs, subtractive color mixing allows the hue of an electrochromic device (ECD) to be

selected and tailored to an application, significantly increasing access to various subtle shades.

The mechanism for production of a visual stimulus in subtractive color mixing, or the production of color through removal of certain wavelengths from a visual stimulus, is the same among a wide range of situations ranging from the colors of paints, dyes, and inks to applications such as electronic paper (ePaper) displays and electrochromic windows. This mechanism is characterized by the interplay between an illuminant or light source, an object to be viewed, and the viewer. This three-way interaction is in contrast to emissive or additive color mixing, where visual stimuli are produced through the interplay of a source and its viewer.

Many non-emissive displays, whether liquid crystal or electrophoretic, are largely black and white or grey scale displays as a result of the nature of their picture elements. With the addition of a yellow-to-transparent material,<sup>3</sup> the ECPs developed in our labs now have the potential to produce full-color non-emissive displays by applying the CMY subtractive mixing model to display elements. Colored-to-transparent electrochromic materials representing these three colors, built into sub-pixel elements, allow for a non-emissive display to exhibit a wider range of colors by means of modulating the

Received: January 14, 2014

Accepted: April 4, 2014

Published: April 21, 2014

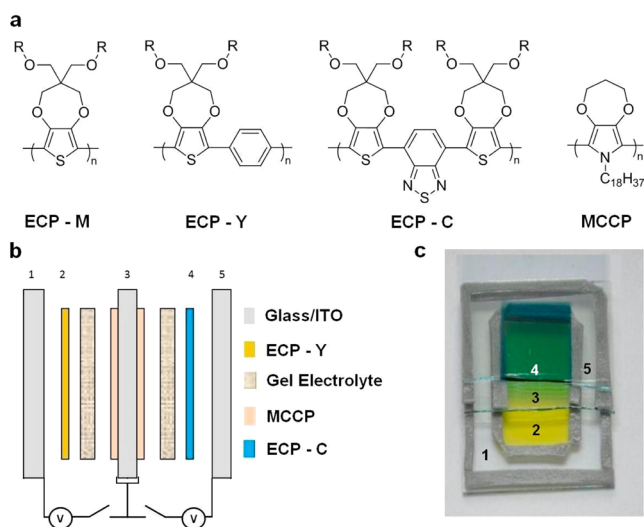


**Figure 1.** (a) Repeat unit structures of ECPs, magenta (-M), yellow (-Y), and cyan (-C), as well as a propylene dioxypyrrole-based minimally color changing polymer (MCCC) ( $R = 2$ -ethylhexyl). (b) Exploded view and (c) photograph of a dual-active ECD, including the voltage control scheme. Working electrodes consist of ITO-coated glass slides (1 and 5) onto which an electrochromic polymer (2 and 4) has been spray-cast. The counter electrode (3) is composed of a double-sided ITO-coated glass slide, of which both sides are coated with spray-cast MCCC.

extent to which various portions of the spectrum are removed from a visual stimulus. This type of device retains many of the benefits associated with non-emissive displays, such as a low power consumption rate, and is potentially mechanically flexible. This idea of color control in light modulation can also be extended to electrochromic windows, wherein a mixture of ECP filters would result in an aesthetically pleasing colored or color-neutral black-to-transmissive window.

Other electrochromic materials, such as small organic molecules like viologen- or phthalate-based materials where subtractive color mixing is demonstrated or inorganic electrochromes, are also available for window and display applications.<sup>8–12</sup> However, the ease and potentially low cost of solution processing in combination with the low switching voltage requirements in ECPs make them attractive materials. Further advantages of ECPs include the presence of bistability in the colored and bleached states because, after removing the voltage used to drive the switch, only a slow change in the optical density occurs at open circuit. Another important consideration of electrochromic materials is the time to fully switch, which is highly application-dependent. When considering active display applications, switching within 100 ms is required, whereas applications such as electronic paper are permissive of sub-second switch times.<sup>13</sup> Further, larger format applications such as signage, informational displays, billboards, mirrors, and windows require switch times no faster than a few to tens of seconds.<sup>14,15</sup> With this, the combination of properties seen in ECPs make them a natural choice for materials to be studied when considering various non-emissive display applications.

Toward this end, a study of subtractive color mixing in ECPs has been carried out using a window-type ECD. Consisting of a pair of optically transparent electrodes encapsulating electrochromic material, window-type devices allow for easy measurement of the optical properties of an ECD while still maintaining

galvano- or potentiostatic control.<sup>8,16–19</sup> These window-type ECDs stand in contrast with reflective-type ECDs that contain a layer of a reflective material, such as  $\text{TiO}_2$  or gold, which have been used in demonstrations of patterning in ECDs.<sup>20–22</sup> One feature of many window-type ECDs is the complementary pairing of cathodically and anodically coloring polymers to provide for charge balance within a device.<sup>23,24</sup> For this, a family of anodically coloring *N*-alkyl-substituted poly(3,4-propylenedioxythiophene) (PProDOT) materials was developed.<sup>25,26</sup> In general, these materials retained residual color in their bleached states, reducing device contrast and transmissivity. What was needed was an anodically coloring electrochromic polymer with little to no absorbance of visible light in either the neutral or oxidized states that still provided for charge balance. Fortunately, PProDOT-*N*- $\text{C}_{18}\text{H}_{37}$ , an octadecyl-*N*-alkylated PProDOT polymer, was seen to display such a behavior.<sup>27</sup> As such, this material is referred to as an MCCC, or minimally color changing polymer (Figure 1a), allowing window-type devices with a distinct colored-to-transparent electrochromic shift to be developed.<sup>28</sup>

Initial studies of color mixing in electrochromic polymers were carried out in electrochemical cells under potential control via a reference electrode, although this concept was soon translated to an electrochromic device.<sup>24,29</sup> With this arrangement, two independently controlled working electrodes are used to set the potential (and thus the color state) of a pair of electrochromic polymers while a single counter electrode is held in common between them. When in an electrochemical cell, this arrangement is referred to as a pseudo-three-electrode setup, although when translated to a device, the name *dual active* has been applied as a description. A diagram of the dual-active-type ECDs employed in the study of subtractive color mixing in ECPs is shown in Figure 1b along with a cutaway photograph of a device in Figure 1c, illustrating the layering of optically transparent electrode substrates and electrochromic polymers.

In the work reported here, we use this dual-active ECD for subtractive color mixing utilizing our ECP-C, ECP-M, and ECP-Y primary system. The bounds of the color gamut, or the subset of accessible colors, using these three PProDOT-derived materials in combination with the recently recognized MCCC polymer have been mapped, highlighting the strengths and weaknesses of employing subtractive color mixing toward the development of full-color non-emissive displays.

## MATERIALS AND METHODS

**Materials.** ECP-C ( $M_n$ , 11.0 kDa; PDI, 1.6), ECP-M ( $M_n$ , 26 kDa; PDI, 1.7), ECP-Y ( $M_n$ , 20 kDa; PDI, 1.7), and MCCC ( $M_n$ , 63 kDa; PDI, 1.7) were synthesized according to previously reported methodologies.<sup>2,3,5,27</sup> Propylene carbonate (99.5% purity) was purchased from Acros Organics, toluene (99.5% purity), from BDH, and chloroform (99.8% purity) and lithium bis-(trifluoromethanesulfonyl)imide (LiTfI) (99% purity), from Alfa Aesar. All reagents were used without further purification. The electrolyte employed in all devices consisted of a propylene carbonate solution containing 0.5 M LiTfI rendered a viscous gel electrolyte via incorporation of 8 wt % high-molecular-weight poly(methyl methacrylate) (PMMA,  $M_w = 960\,000$  g/mol), which was purchased from Aldrich. ITO-coated glass slides ( $25 \times 75 \times 0.7$  mm<sup>3</sup>, sheet resistance 5–15  $\Omega$ /sq) were purchased from Delta Technologies, Ltd. Polymer solutions at a concentration of 2 mg/mL were made in toluene or in a 1:1 (v/v) toluene/chloroform mixture in the case of ECP-C. Polymer solutions were passed through 0.45  $\mu\text{m}$  PTFE syringe filters purchased from Tisch and cast using an Iwata-Eclipse HP-BC airbrush with argon at a pressure of 20 psi.

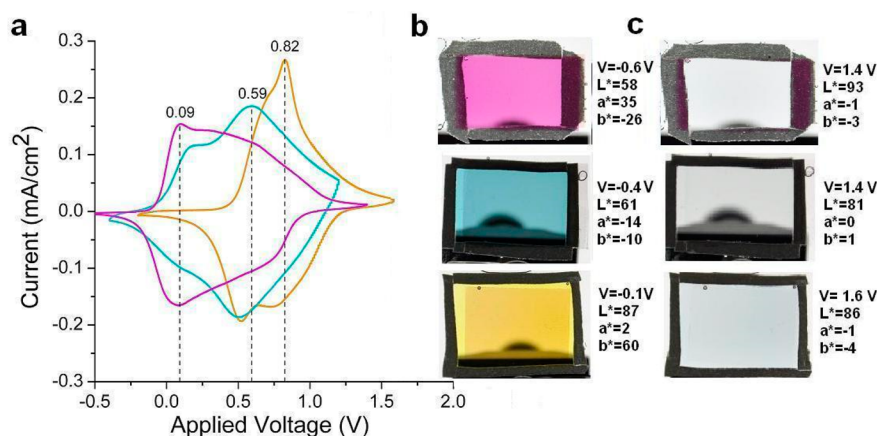


**Figure 2.** (a) Cyclic voltammetry and (b) colored and (c) bleached state photographs of ECP-M (magenta), -C (cyan), and -Y (yellow) in dual-film ECDs with MCCP. Cyclic voltammetry was performed with 0.5 M LiBTI/PC gel electrolyte at a scan rate of 75 mV/s. The photographed devices were broken in by cycling the applied voltage within a range appropriate for each ECP 3–5 times. The voltage ranges for devices utilizing ECP-M, -C, and -Y are  $-0.6$  to  $1.4$  V,  $-0.4$  to  $1.2$  V, and  $-0.2$  to  $1.6$  V, respectively. At the end of the break-in period, a stable current response on further cycling is observed.

**Film Characterization.** Films were cast until an optical density of 0.8 absorbance units (a.u.) at  $\lambda_{\text{max}}$  or 0.4 a.u. in the case of MCCP, as monitored on a Varian Cary 5000 UV–vis–NIR spectrophotometer, was reached. Each film was sprayed over an area measuring  $1.2 \times 1.7$  cm<sup>2</sup>. Because the optical properties of the materials employed are the focus of the present study, optical density in the form of absorbance units was selected as the basis on which to compare films as opposed to a more standard thin film measure such as film thickness.

**Device Characterization.** To construct the dual-active ECDs, ECP films were first spray-cast onto ITO-coated glass substrates to the appropriate optical density. Two borders were created using strips of VHB foam acrylic tape (series 4926, 3M): the first border was placed around the ECP films cast onto the center of the substrate and then a second border was placed around the outer edges of the substrates, which is shown in Figure 1c (gray gasket). The gel electrolyte mixture was transferred into the reservoir created by the tape, and the counter electrode slide was placed on top. The process of creating borders of VHB tape around the edges of both the cast ECP and ITO-coated glass substrate, followed by the addition and encapsulation of gel electrolyte, was repeated on the reverse side of the double-sided ITO-coated glass slide used as the counter electrode layer to add the second ECD portion and to create the completed device. Contact was made to the devices using  $1/2$  inch EMI shielding copper tape (series 1181, 3M). Cyclic voltammetry was carried out using an EG&G PAR 273A potentiostat/galvanostat under CorrWare control. Independent voltage control of the two working electrodes of each device was attained via Pine AFCBP1 bipotentiostats, controlled via AfterMath Scientific Data Organizer software. Spectroelectrochemistry was carried out on a Varian Cary 5000 UV–vis–NIR spectrophotometer. Colorimetry measurements were performed with a Minolta CS-100 chroma meter. Samples for colorimetric analysis were measured using the CIE recommended normal/normal (0/0) illuminating/viewing geometry for transmittance measurements, and each sample was illuminated in a light booth by a D50 (5000 K) lamp. Photography was performed in this light booth, with D50 illumination, using a Nikon D90 SLR camera with a Nikon 18-105 mm VR lens and is reported without further manipulation beyond photograph cropping.

## RESULTS AND DISCUSSION

Cyclic voltammetry was used to establish stable switching voltages for each ECP-MCCP pairing. Cyclic voltammograms for individual (i.e., not dual-active) ECDs utilizing ECP-M, ECP-C, and ECP-Y as the working electrode materials and MCCP as the counter electrode material are shown in Figure 2a. The windows established were  $-0.6$  to  $1.4$  V,  $-0.4$  to  $1.2$  V,

and  $-0.2$  to  $1.6$  V for magenta, cyan, and yellow ECDs, respectively. Owing to the construction of the dual-active device that allowed each working electrode to be controlled independently, the voltage windows established with these ECDs are translatable to the dual-active architecture. Freshly constructed ECDs must be switched until a steady current response is observed by cycling the applied voltage within the established voltage window several times. This break-in period is commonly observed and reflects the redox and structural changes occurring throughout the polymer during full ion–solvent permeation into the films.<sup>30</sup> Shown in Figure 2, panels b and c are photographs of the individual color ECDs in their colored and bleached states alongside the CIELAB (CIE  $L^*a^*b^*$ ) colorimetric coordinates. CIELAB is a tricoordinate system used to quantify color, where  $L^*$  represents the white–black balance,  $a^*$  represents green–red balance, and  $b^*$  represents the blue–yellow balance of a given color.<sup>31</sup> Higher  $a^*b^*$  values correspond to higher color saturation, whereas the  $L^*$  coordinate, scaling from 0–100, represents the lightness or darkness of a hue.

As an example, the coordinates shown for the yellow device in Figure 2b ( $L^* = 87$ ,  $a^* = 2$ ,  $b^* = 60$ ), represents a bright, saturated yellow color. This saturated color is converted to a low saturation and transmissive color-neutral bleached state, shown in Figure 2c, with coordinates (86,  $-1$ ,  $-4$ ) when ECP-Y is oxidized. This saturated-to-unsaturated (colored-to-transmissive) transition can be seen in each of the three devices examined in Figure 2, demonstrating high contrast switching at relatively low voltages and making them useful for the study of color mixing. Spectroelectrochemical series, colorimetric data, and additional photographs of the devices shown in Figure 2 can be found in the Supporting Information (Figure S1).

Initial color mixing experiments were performed using a simple stacked device architecture that lacked the central double-sided counter electrode (layer 3 in Figure 1b,c) and was instead composed of two independent ECDs, of the type shown in Figure 2, placed back to back. To gain a better view of how color mixing is achieved in both the dual-active and stacked devices, each side might be envisioned as a tunable filter. The two ECP films in series will absorb a portion of the light from the illuminant before reaching an observer, producing a mixed color stimulus. Tuning these ECP filters is

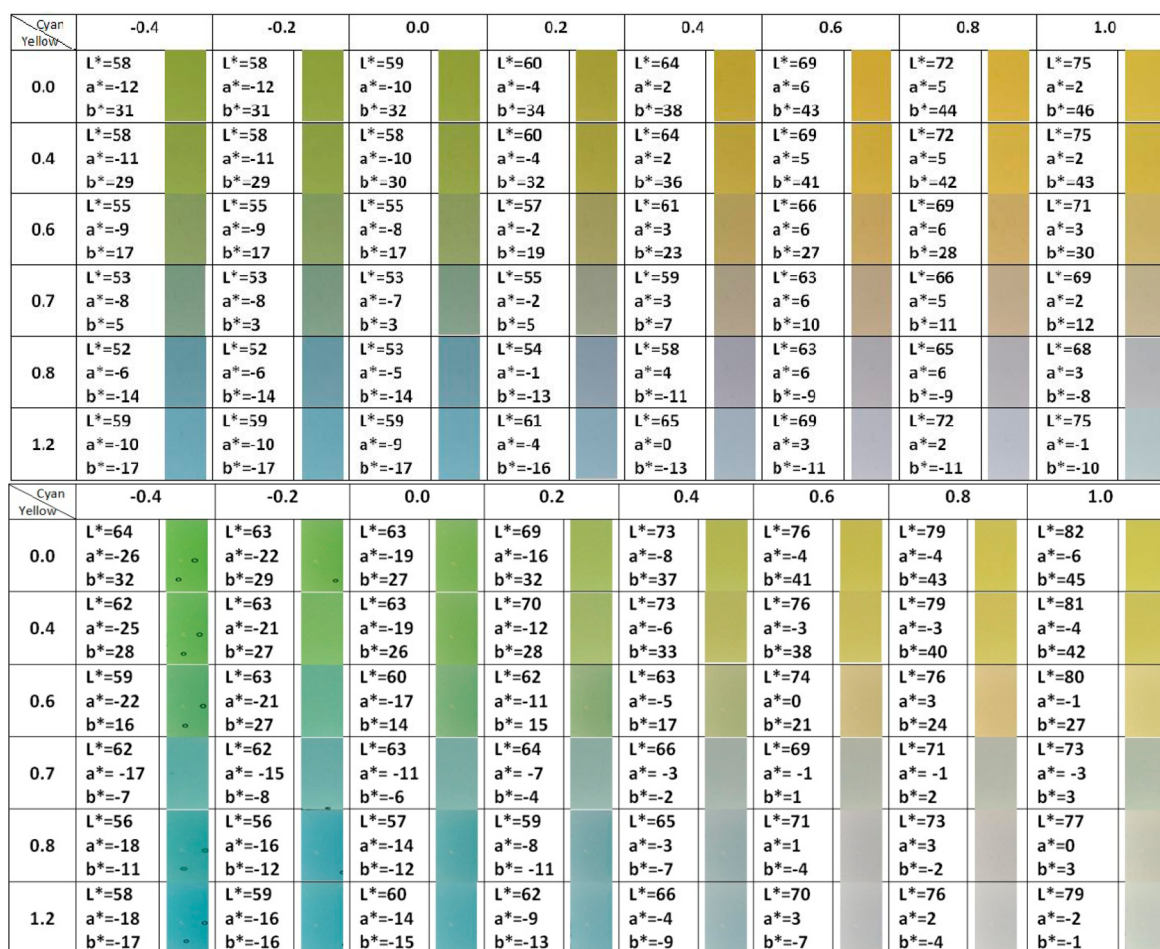


**Figure 3.** Comparison of the color states in stacked (top) and dual-active (bottom) cyan + yellow ECDs. Photographs are shown alongside the  $L^*a^*b^*$  coordinates corresponding to the accessed color and the applied voltages at which that color is accessed. Values shown here are a sampling of the total number of available color states, of which all can be accessed through finer control of the applied voltage. Note that the circles appearing in photographs of the lower color table are air bubbles trapped in the gel electrolyte layer of the device.

accomplished by independently controlling the voltage applied to each device, decreasing light absorption in the visual region as each ECP is oxidized.

Unlike a simple filter, the construction of both dual-active and stacked devices includes a number of optical interfaces (e.g., air to glass, glass to ITO, etc.) that also play a role in the spectral profile of light reaching an observer.<sup>32</sup> The influence of these interfaces in the stacked device structure on color properties is illustrated in Figure 3, which compares the color states accessible in a cyan + yellow (green) stacked device (top) with the corresponding dual-active structure (bottom). The color gamut produced in each architecture was probed by gradually increasing the voltages applied across each film and recording a photograph and the colorimetric data of the mixed color stimuli as a function of these two applied voltages. The differences in the two device architectures are visually apparent via the photographs, with the stacked device shown in the upper half of Figure 3 exhibiting muted, or less saturated, color states. The  $L^*a^*b^*$  coordinates associated with each color state can then be used to quantitatively demonstrate the larger degree of color saturation seen in the dual-active structure via the equation

$$S_{ab} = \frac{C_{ab}^*}{\sqrt{C_{ab}^{*2} + L^{*2}}} 100\% = \frac{\sqrt{a^{*2} + b^{*2}}}{\sqrt{C_{ab}^{*2} + L^{*2}}} 100\% \quad (1)$$

where color saturation ( $S_{ab}$ ) is the ratio of chromatic color ( $C_{ab}^*$ ) to the total color sensation.<sup>33,34</sup> As shown in Table 1,

**Table 1. Comparison of Saturation Values in the Dual-Active and Stacked Devices Shown in Figure 3**

color state	$S_{ab}$ (dual active)	$S_{ab}$ (stacked)
green	54	49
cyan	39	31
yellow	48	52
transmissive	2	13

using this measure to compare the saturation of the color states at the four color extreme corners of Figure 3 (green, cyan, yellow, and transmissive color states), higher degrees of saturation are observed in the green and cyan states of the dual-active device relative to the stacked device. Furthermore, the color saturation of the transmissive state in the dual-active device is seen to be lower than that of the stacked device, indicating that a more color-neutral and transmissive bleached state is produced using the dual-active device.

Magenta Cyan	-0.6	-0.4	-0.2	0.0	0.2	0.4	0.6	0.8
-0.2	L*=39 a*=14 b*=-29	L*=40 a*=13 b*=-28	L*=46 a*=7 b*=-18	L*=54 a*=-3 b*=-11	L*=56 a*=-5 b*=-11	L*=57 a*=-6 b*=-12	L*=58 a*=-6 b*=-15	L*=59 a*=-7 b*=-16
0.0	L*=41 a*=17 b*=-27	L*=42 a*=17 b*=-27	L*=47 a*=12 b*=-19	L*=54 a*=4 b*=-10	L*=57 a*=-1 b*=-9	L*=58 a*=-1 b*=-11	L*=59 a*=-3 b*=-14	L*=60 a*=-4 b*=-15
0.2	L*=42 a*=23 b*=-26	L*=42 a*=23 b*=-25	L*=45 a*=22 b*=-22	L*=54 a*=13 b*=-8	L*=59 a*=7 b*=-5	L*=60 a*=5 b*=-7	L*=62 a*=3 b*=-10	L*=63 a*=2 b*=-12
0.4	L*=46 a*=29 b*=-20	L*=46 a*=29 b*=-20	L*=48 a*=28 b*=-17	L*=58 a*=19 b*=-2	L*=62 a*=13 b*=2	L*=64 a*=11 b*=0	L*=66 a*=9 b*=-3	L*=67 a*=9 b*=-5
0.6	L*=48 a*=32 b*=-17	L*=48 a*=32 b*=-17	L*=49 a*=31 b*=-16	L*=59 a*=23 b*=0	L*=65 a*=16 b*=5	L*=67 a*=13 b*=3	L*=69 a*=11 b*=0	L*=70 a*=11 b*=-2
0.8	L*=49 a*=32 b*=-18	L*=49 a*=32 b*=-18	L*=50 a*=31 b*=-17	L*=60 a*=25 b*=-2	L*=66 a*=17 b*=4	L*=68 a*=14 b*=2	L*=70 a*=12 b*=-1	L*=71 a*=12 b*=-3

Magenta Yellow	-0.6	-0.4	-0.2	0.0	0.2	0.4	0.6	0.8
0.2	L*=57 a*=22 b*=27	L*=59 a*=26 b*=26	L*=66 a*=21 b*=33	L*=72 a*=13 b*=40	L*=75 a*=10 b*=43	L*=78 a*=8 b*=41	L*=78 a*=8 b*=39	L*=81 a*=4 b*=36
0.4	L*=56 a*=23 b*=24	L*=59 a*=26 b*=26	L*=66 a*=21 b*=34	L*=72 a*=13 b*=40	L*=75 a*=10 b*=43	L*=78 a*=8 b*=41	L*=78 a*=8 b*=40	L*=81 a*=4 b*=36
0.6	L*=53 a*=22 b*=8	L*=58 a*=25 b*=21	L*=63 a*=20 b*=17	L*=69 a*=12 b*=26	L*=74 a*=10 b*=39	L*=76 a*=7 b*=33	L*=77 a*=8 b*=37	L*=79 a*=4 b*=26
0.7	L*=51 a*=21 b*=-8	L*=56 a*=23 b*=7	L*=61 a*=19 b*=7	L*=67 a*=11 b*=11	L*=71 a*=8 b*=26	L*=73 a*=7 b*=15	L*=75 a*=6 b*=25	L*=76 a*=4 b*=11
0.8	L*=51 a*=25 b*=-16	L*=54 a*=23 b*=-13	L*=61 a*=18 b*=-3	L*=67 a*=10 b*=5	L*=69 a*=7 b*=4	L*=72 a*=6 b*=8	L*=73 a*=5 b*=4	L*=76 a*=3 b*=4
1.0	L*=54 a*=28 b*=-18	L*=56 a*=26 b*=-19	L*=63 a*=20 b*=-10	L*=69 a*=11 b*=-3	L*=71 a*=9 b*=-2	L*=75 a*=5 b*=-1	L*=75 a*=5 b*=-5	L*=78 a*=1 b*=-7
1.2	L*=57 a*=27 b*=-20	L*=58 a*=27 b*=-18	L*=65 a*=19 b*=-9	L*=71 a*=10 b*=-2	L*=74 a*=8 b*=-1	L*=77 a*=4 b*=0	L*=77 a*=4 b*=-5	L*=79 a*=1 b*=-6

**Figure 4.** Examination of the gamut of color states in dual-active magenta + cyan (top) and magenta + yellow (bottom) devices. Again, a sampling of available color states is shown, with a focus toward the four extremes. With these additions, all quadrants of the  $L^*a^*b^*$  color space become accessible, allowing for a full and high-resolution color gamut to be observed.

Interestingly, a higher degree of yellow saturation is observed in the stacked rather than the dual-active device, although the difference is slight. The results shown in Figures 3 and 4 further emphasize the tunable nature of the color states exhibited by the ECPs used in the device construction, with each color state readily accessed via the application of a specific pair of voltages across each portion of the device.

In addition to the comparison of saturation values between devices, comparison of the  $L^*a^*b^*$  coordinates of the colors produced in the ECDs with color standards commonly perceived as saturated colors, such as those of the Munsell color checker system, can be used to gauge the performance of color production.<sup>35</sup> Although other color standards exist, such as the Pantone system, the Munsell color system is based on the human perception of color, whereas most other systems are intended for use in textile dyeing or printing settings. The ability to match colors can be quantified through the value of  $\Delta E_{ab}$ , which is the color difference or the distance between two points in a color space. In the CIELAB color space, this value is calculated via the equation

$$\Delta E_{ab}^* = \sqrt{(L_2^* - L_1^*)^2 + (a_2^* - a_1^*)^2 + (b_2^* - b_1^*)^2} \quad (2)$$

When comparing the green states of the dual-active and stacked devices in Figure 3 with Munsell green (which has  $L^*a^*b^*$  coordinates of 55,38,31), the value of  $\Delta E_{ab}$  is determined to be 50 in the stacked device but only 15 in the dual-active device. This smaller color difference in the dual-active device indicates that it better matches a hue commonly accepted as green to the casual observer. The ability of the dual-active device to produce more saturated shades that better match color standards extends to the cyan ( $\Delta E_{ab} = 16$  in dual active and  $\Delta E_{ab} = 23$  in stacked vs Munsell cyan) state as well, although both devices are nearly equal in their ability to match the Munsell standard yellow ( $\Delta E_{ab} = 36$  in dual active and  $\Delta E_{ab} = 35$  in stacked). These measures of performance and higher values of color saturation as well as the ability to produce less muddled shades that more accurately match color standards indicate that the dual-active device architecture is a preferable model to use in ECD color mixing studies.

We have demonstrated here that green and its primary colors are well-represented with a dual-active device, but a full-color display needs more than just variations of green. If colors ranging from oranges to yellows and purples to blues are to be generated, then the color mixing of other primary pairs is necessary. For this reason, dual-active devices with cyan–magenta (top) and magenta–yellow (bottom) combinations were constructed and characterized, as illustrated by the photographic and colorimetric results shown in Figure 4.

Although this device does produce blue tones, the coordinates of the fully neutral state of this device (cyan,  $-0.2$  V; magenta,  $-0.4$  V) are closer to a purple than a blue with a  $\Delta E_{ab}$  of 14 versus Munsell purple as compared to the  $\Delta E_{ab}$  of 23 versus Munsell blue. This shift in the secondary color, moving from blue to purple, is likely due to the difference in saturation of the films used. The color saturation ( $S_{ab}$ ) in an ECP cyan device shown in Figure 2b is 27, as compared to the magenta device also shown in Figure 2b, for which  $S_{ab} = 60$ . A similar disparity in the saturation of the constituent ECP films of the magenta–yellow device in Figure 4 lends to the orange hue of the fully neutral color state. This difference in saturation could be overcome by, in the case of the cyan–magenta device, increasing the thickness of the deposited cyan film, thereby increasing the chromaticity and saturation of that component. However, the optical density of the films employed in devices were set to be equal to one another for the purposes of this investigation.<sup>36</sup> What is evident from Figures 3 and 4 is the ability to dial in a color state by applying a set of particular voltages across the two halves of a dual-active ECD.

Taken together, the breadth of the color states accessed using these dual-active devices form a color gamut, particularly for these ECP materials at a specific optical density. This gamut, shown plotted in the  $a^*b^*$  color space in Figure 5, is, to our

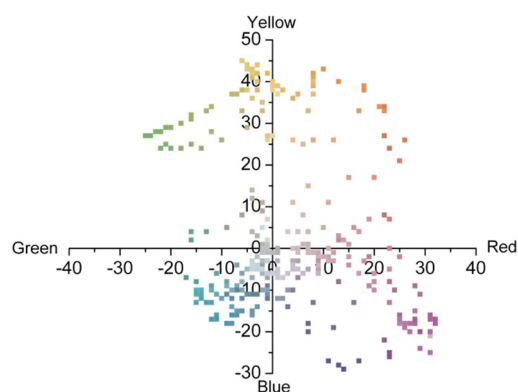


**Figure 5.** Plot of  $a^*b^*$  values of all color points recorded with dual-active devices. This plot shows that a large range of color states can be generated in the subtractive color mixing of electrochromic polymers. The color of the points shown is not photographic but rather is RGB color mapping produced from the corresponding  $L^*a^*b^*$  coordinates. Variations in  $L^*$  values are not explicitly shown.

knowledge, the first of its kind to be produced using subtractive color mixing in electrochromic polymers, where the color points shown correspond to the color points from Figures 3 and 4.

This gamut, plotted as if all points were of equal  $L^*$  value, shows a broad range of accessible color states. The coloration of points shown in Figure 5 is not from photographs of devices, as is the case in Figures 3 and 4; rather, it is a color mapping

performed during data workup by converting the  $L^*a^*b^*$  coordinates for each point to RGB values. It should be noted that the space between the plotted points, or the color resolution of the displayed gamut, is a function of the voltages applied to the dual-active device. These measurements were made utilizing 200 mV steps throughout stable switching ranges. By utilizing smaller voltage steps, additional color states not shown can be accessed. The only exception to this voltage stepping regime is in the case of ECP-Y films that include an oddly spaced point at 0.7 V, which was included because of the large degree of change that occurs at this voltage in order to illustrate a more smooth transition.

If a finer control of the applied voltages can serve to fill in the accessible color states of the gamut, then the features of greatest interest become the color states with the greatest chromaticity, or the points that make up the outer bounds of the gamut. These boundaries, shown in Figure 6, reflect the limits of color production in these materials at the specific optical density examined.

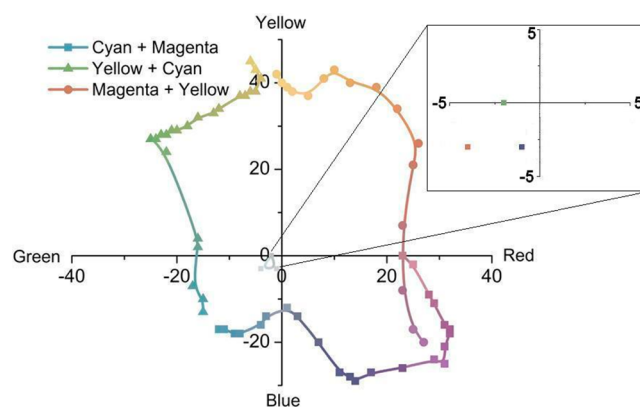


**Figure 6.** Exterior and interior bounds of the color gamut generated through subtractive mixing of ECP-M, -Y, and -C. Values in the green and blue borders are lacking owing to the weak color contribution from the cyan primary, whereas strong yellow and magenta primaries lead to a large area of available color points. Not all devices are created equally though, as shown by the disparity in the magenta border laid out by cyan + magenta and magenta + yellow. Inset: points corresponding to fully bleached states of green, blue, and red dual-active devices.

A number of points are brought up by the examination of boundaries of the accessed color gamut. First, the borders displayed include a tail in the lower right quadrant, shown to be from the magenta + yellow device. The reason for the inclusion of this tail is to demonstrate variability between devices. Given the variability inherent in lab-built devices, these bounds can be expected to fluctuate to a certain extent with the assembly of each device, and with a sufficient number of devices, this variability would likely average out. Second, although there is variation from device to device, each dual-active device can achieve a very transmissive state. This is provided in the inset to Figure 6, which shows the coordinates for each of the dual-active devices with the ECPs in their fully oxidized states. Third, although points are plotted in accordance with their  $a^*b^*$  values, a third dimension ( $L^*$ ) is not represented, save for the coloring of plotted points. If the  $L^*$  dimension was taken into account in plotting, then the mapped gamut would appear as an ovoid shape in the  $L^*a^*b^*$  color space, with an apex toward the yellow and a nadir in the purple–blue region, rather

than a distorted circle. Consideration of this third  $L^*$  dimension brings up another point of interest. Although precise control over the  $a^*b^*$  color state has been demonstrated utilizing this type of dual-active ECD, variation in  $L^*$  occurs as a consequence of the bleaching and evocation of color in the ECPs used. No direct control over the lightness or darkness of the color states produced using a dual-active device is present.

To address the absence of control over the white–black balance in this type of device, a fourth “ECP-Black” component could also be incorporated into a hypothetical pixel, varying in shades of black.<sup>37</sup> This practice is common in printing, where the subtractive color mixing system employed here is almost exclusively referred to as CMY-K, with K being short for *key*, a press-printing term for black. Direct control over the  $L^*$  value would allow for further expansion of this three-dimensional color gamut, permitting access to color states otherwise precluded by the bleaching of the cyan, magenta, and yellow ECPs. With the incorporation of this fourth element to control luminosity of mixed colors, the concern once again becomes the ability of the ECPs to produce a wide gamut of saturated color states. If the bounds laid out by the saturation of the primaries are of concern instead, then one source of limitation is plain to see in Figure 6, namely, the lack of saturation in the cyan primary.

In summary, it has been demonstrated here that ECPs are suitable for the generation of a wide gamut of colors through secondary mixing when layered as two distinct films, exhibiting both vibrantly colored and highly transmissive states in equal measure. In addition, color states may be selectively tuned as intermediate partially bleached color states readily accessed by the judicious application of voltages. The large number of distinct color states accessible through this partial oxidation of ECP materials, in either individual films or when coupled as two or more tunable filters, results in a wide color gamut encompassing a considerable variety of color permutations within its bounds.

## ■ ASSOCIATED CONTENT

### Supporting Information

Spectroelectrochemical series, the associated colorimetric data, and colored and bleached state photographs of ECDs composed of MCCP paired with either ECP-M, -Y, or -C. This material is available free of charge via the Internet at <http://pubs.acs.org>.

## ■ AUTHOR INFORMATION

### Corresponding Author

\*E-mail: [reynolds@chemistry.gatech.edu](mailto:reynolds@chemistry.gatech.edu).

### Notes

The authors declare no competing financial interest.

## ■ ACKNOWLEDGMENTS

We thank BASF for funding. We also thank Dr. Michael Craig for the synthesis and purification of ECP-M, ECP-C, and MCCP.

## ■ REFERENCES

- (1) Dyer, A. L.; Thompson, E. J.; Reynolds, J. R. Completing the Color Palette with Spray-Processable Polymer Electrochromics. *ACS Appl. Mater. Interfaces* **2011**, *3*, 1787–1795.
- (2) Reeves, B. D.; Grenier, C. R. G.; Argun, A. A.; Cirpan, A.; McCarley, T. D.; Reynolds, J. R. Spray Coatable Electrochromic

Dioxythiophene Polymers with High Coloration Efficiencies. *Macromolecules* **2004**, *37*, 7559–7569.

- (3) Amb, C. M.; Kerszulis, J. A.; Thompson, E. J.; Dyer, A. L.; Reynolds, J. R. Propylenedioxythiophene (ProDOT)–Phenylene Copolymers Allow a Yellow-to-Transmissive Electrochrome. *Polym. Chem.* **2011**, *2*, 812–814.

- (4) Beaujuge, P. M.; Ellinger, S.; Reynolds, J. R. Spray Processable Green to Highly Transmissive Electrochromics via Chemically Polymerizable Donor–Acceptor Heterocyclic Pentamers. *Adv. Mater.* **2008**, *20*, 2772–2776.

- (5) Beaujuge, P. M.; Amb, C. M.; Reynolds, J. R. Spectral Engineering in  $\pi$ -Conjugated Polymers with Intramolecular Donor–Acceptor Interactions. *Acc. Chem. Res.* **2010**, *43*, 1396–1407.

- (6) Amb, C. M.; Beaujuge, P. M.; Reynolds, J. R. Spray-Processable Blue-to-Highly Transmissive Switching Polymer Electrochromes via the Donor–Acceptor Approach. *Adv. Mater.* **2010**, *22*, 724–728.

- (7) Amb, C. M.; Dyer, A. L.; Reynolds, J. R. Navigating the Color Palette of Solution-Processable Electrochromic Polymers. *Chem. Mater.* **2010**, *23*, 397–415.

- (8) Monk, P. M. S.; Mortimer, R. J.; Rosseinsky, D. R. *Electrochromism and Electrochromic Devices*, 2nd ed; Cambridge University Press: Cambridge, 2007.

- (9) Granqvist, C. G. Electrochromic Tungsten Oxide Films: Review of Progress 1993–1998. *Sol. Energy Mater. Sol. Cells* **2000**, *60*, 201–262.

- (10) Watanabe, Y.; Nagashima, T.; Nakamura, K.; Kobayashi, N. Continuous-Tone Images Obtained Using Three Primary-Color Electrochromic Cells Containing Gel Electrolyte. *Sol. Energy Mater. Sol. Cells* **2012**, *104*, 140–145.

- (11) Costa, C.; Pinheiro, C.; Henriques, I.; Laia, C. A. T. Electrochromic Properties of Inkjet Printed Vanadium Oxide Gel on Flexible Polyethylene Terephthalate/Indium Tin Oxide Electrodes. *ACS Appl. Mater. Interfaces* **2012**, *4*, 5266–5275.

- (12) Monk, P. M. S.; Delage, F.; Costa Vieira, S. M. Electrochromic Paper: Utility of Electrochromes Incorporated in Paper. *Electrochim. Acta* **2001**, *46*, 2195–2202.

- (13) Sun, X. W.; Wang, J. X. Fast Switching Electrochromic Display Using a Viologen-Modified ZnO Nanowire Array Electrode. *Nano Lett.* **2008**, *8*, 1884–1889.

- (14) Yang, X.; Zhu, G.; Wang, S.; Zhang, R.; Lin, L.; Wu, W.; Wang, Z. L. A Self-Powered Electrochromic Device Driven by a Nanogenerator. *Energy Environ. Sci.* **2012**, *5*, 9462–9466.

- (15) Choi, S. Y.; Mamak, M.; Coombs, N.; Chopra, N.; Ozin, G. A. Electrochromic Performance of Viologen-Modified Periodic Mesoporous Nanocrystalline Anatase Electrodes. *Nano Lett.* **2004**, *4*, 1231–1235.

- (16) Beaupré, S.; Breton, A.-C.; Dumas, J.; Leclerc, M. Multicolored Electrochromic Cells Based on Poly(2,7-carbazole) Derivatives for Adaptive Camouflage. *Chem. Mater.* **2009**, *21*, 1504–1513.

- (17) Kobayashi, N.; Miura, S.; Nishimura, M.; Urano, H. Organic Electrochromism for a New Color Electronic Paper. *Sol. Energy Mater. Sol. Cells* **2008**, *92*, 136–139.

- (18) Rauh, R. D.; Wang, F.; Reynolds, J. R.; Meeker, D. L. High Coloration Efficiency Electrochromics and Their Application to Multi-Color Devices. *Electrochim. Acta* **2001**, *46*, 2023–2029.

- (19) Schwendeman, I.; Hwang, J.; Welsh, D. M.; Tanner, D. B.; Reynolds, J. R. Combined Visible and Infrared Electrochromism Using Dual Polymer Devices. *Adv. Mater.* **2001**, *13*, 634–637.

- (20) Argun, A. A.; Berard, M.; Aubert, P. H.; Reynolds, J. R. Back-Side Electrical Contacts for Patterned Electrochromic Devices on Porous Substrates. *Adv. Mater.* **2005**, *17*, 422–426.

- (21) Argun, A. A.; Reynolds, J. R. Line Patterning for Flexible and Laterally Configured Electrochromic Devices. *J. Mater. Chem.* **2005**, *15*, 1793–1800.

- (22) Aubert, P.-H.; Argun, A. A.; Cirpan, A.; Tanner, D. B.; Reynolds, J. R. Microporous Patterned Electrodes for Color-Matched Electrochromic Polymer Displays. *Chem. Mater.* **2004**, *16*, 2386–2393.

- (23) Nikolou, M.; Dyer, A. L.; Steckler, T. T.; Donoghue, E. P.; Wu, Z.; Heston, N. C.; Rinzler, A. G.; Tanner, D. B.; Reynolds, J. R. Dual

n- and p-Type Dopable Electrochromic Devices Employing Transparent Carbon Nanotube Electrodes. *Chem. Mater.* **2009**, *21*, 5539–5547.

(24) Unur, E.; Beaujuge, P. M.; Ellinger, S.; Jung, J.-H.; Reynolds, J. R. Black to Transmissive Switching in a Pseudo Three-Electrode Electrochromic Device. *Chem. Mater.* **2009**, *21*, 5145–5153.

(25) Walczak, R. M.; Leonard, J. K.; Reynolds, J. R. Processable, Electroactive, and Aqueous Compatible Poly(3,4-alkylenedioxythiophene)s through a Functionally Tolerant Deiodination Condensation Polymerization. *Macromolecules* **2008**, *41*, 691–700.

(26) Walczak, R.M.; Reynolds, J. R. Poly(3,4-alkylenedioxythiophenes): The PxDOPs as Versatile Yet Underutilized Electroactive and Conducting Polymers. *Adv. Mater.* **2006**, *18*, 1121–1131.

(27) Knott, E. P.; Craig, M. R.; Liu, D. Y.; Babiarz, J. E.; Dyer, A. L.; Reynolds, J. R. A Minimally Coloured Dioxypyrrrole Polymer as a Counter Electrode Material in Polymeric Electrochromic Window Devices. *J. Mater. Chem.* **2012**, *22*, 4953–4962.

(28) Vasilyeva, S. V.; Beaujuge, P. M.; Wang, S.; Babiarz, J. E.; Ballarotto, V. W.; Reynolds, J. R. Material Strategies for Black-to-Transmissive Window-Type Polymer Electrochromic Devices. *ACS Appl. Mater. Interfaces* **2011**, *3*, 1022–1032.

(29) Unur, E.; Jung, J.-H.; Mortimer, R. J.; Reynolds, J. R. Dual-Polymer Electrochromic Film Characterization Using Bipotentiostatic Control. *Chem. Mater.* **2008**, *20*, 2328–2334.

(30) Dyer, A. L.; Craig, M. R.; Babiarz, J. E.; Kiyak, K.; Reynolds, J. R. Orange and Red to Transmissive Electrochromic Polymers Based on Electron-Rich Dioxothiophenes. *Macromolecules* **2010**, *43*, 4460–4467.

(31) *CIE Technical Report: Colorimetry*; Commission Internationale De L'eclairage: Vienna, Austria, 2004.

(32) Hwang, J.; Tanner, D. B.; Schwendeman, I.; Reynolds, J. R. Optical Properties of Nondegenerate Ground-State Polymers: Three Dioxothiophene-Based Conjugated Polymers. *Phys. Rev. B* **2003**, *67*, 1–10.

(33) *The Focal Encyclopedia of Photography*, 3rd ed; Stroebel, L. D., Zakia, R. D., Eds.; Focal Press: Boston, MA, 1993.

(34) Lübke, E. *Farbe im Kopf – Farbsysteme in der Realität*; Muster-Schmidt Verlag: Berlin, Germany, 2008.

(35) Munsell, A. H. A Pigment Color System and Notation. *Am. J. Psychol.* **1912**, *23*, 236–244.

(36) Mortimer, R. J.; Graham, K. R.; Grenier, C. R. G.; Reynolds, J. R. Influence of the Film Thickness and Morphology on the Colorimetric Properties of Spray-Coated Electrochromic Disubstituted 3,4-Propylenedioxythiophene Polymers. *ACS Appl. Mater. Interfaces* **2009**, *1*, 2269–2276.

(37) Shi, P.; Amb, C. M.; Knott, E. P.; Thompson, E. J.; Liu, D. Y.; Mei, J.; Dyer, A. L.; Reynolds, J. R. Broadly Absorbing Black to Transmissive Switching Electrochromic Polymers. *Adv. Mater.* **2010**, *22*, 4949–4953.